

# Supplementary Materials for “Personalized Biopsies in Prostate Cancer Active Surveillance”

Anirudh Tomer, MSc<sup>a,\*</sup>, Daan Nieboer, MSc<sup>b</sup>, Monique J. Roobol, PhD<sup>c</sup>, Anders Bjartell, PhD<sup>d</sup>, Ewout W. Steyerberg, PhD<sup>b,e</sup>, Dimitris Rizopoulos, PhD<sup>a</sup>, Movember Foundations Global Action Plan Prostate Cancer Active Surveillance (GAP3) consortium<sup>f</sup>

<sup>a</sup>*Department of Biostatistics, Erasmus University Medical Center, Rotterdam, the Netherlands*

<sup>b</sup>*Department of Public Health, Erasmus University Medical Center, Rotterdam, the Netherlands*

<sup>c</sup>*Department of Urology, Erasmus University Medical Center, Rotterdam, the Netherlands*

<sup>d</sup>*Department of Urology, Skåne University Hospital, Malmö, Sweden*

<sup>e</sup>*Department of Biomedical Data Sciences, Leiden University Medical Center, Leiden, the Netherlands*

<sup>f</sup>*The Movember Foundations Global Action Plan Prostate Cancer Active Surveillance (GAP3) consortium members presented in Appendix A*

---

---

## 1 Appendix A. A Joint Model for the Longitudinal PSA, and Time 2 to Gleason Reclassification

3 Let  $T_i^*$  denote the true time of reclassification (increase in biopsy Gleason  
4 grade from 1 to 2 or higher) for the  $i$ -th patient included in PRIAS. Since  
5 biopsies are conducted periodically,  $T_i^*$  is observed with interval censoring  
6  $l_i < T_i^* \leq r_i$ . When reclassification is observed for the patient at his latest  
7 biopsy time  $r_i$ , then  $l_i$  denotes the time of the second latest biopsy. Oth-  
8 erwise,  $l_i$  denotes the time of the latest biopsy and  $r_i = \infty$ . Let  $\mathbf{y}_i$  denote

---

\*Corresponding author (Anirudh Tomer): Erasmus MC, kamer flex Na-2823, PO Box 2040, 3000 CA Rotterdam, the Netherlands. Tel: +31 10 70 43393

*Email addresses:* [a.tomer@erasmusmc.nl](mailto:a.tomer@erasmusmc.nl) (Anirudh Tomer, MSc),  
[d.nieboer@erasmusmc.nl](mailto:d.nieboer@erasmusmc.nl) (Daan Nieboer, MSc), [m.roobol@erasmusmc.nl](mailto:m.roobol@erasmusmc.nl) (Monique J. Roobol, PhD), [anders.bjartell@med.lu.se](mailto:anders.bjartell@med.lu.se) (Anders Bjartell, PhD),  
[e.w.steyerberg@lumc.nl](mailto:e.w.steyerberg@lumc.nl) (Ewout W. Steyerberg, PhD), [d.rizopoulos@erasmusmc.nl](mailto:d.rizopoulos@erasmusmc.nl) (Dimitris Rizopoulos, PhD)

his observed PSA longitudinal measurements. The observed data of all  $n$  patients is denoted by  $\mathcal{D}_n = \{l_i, r_i, \mathbf{y}_i; i = 1, \dots, n\}$ .

In our joint model, the patient-specific PSA measurements over time are modeled using a linear mixed effects sub-model. It is given by (see Panel A, Figure 1):

$$\begin{aligned} \log_2 \{y_i(t) + 1\} &= m_i(t) + \varepsilon_i(t), \\ m_i(t) &= \beta_0 + b_{0i} + \sum_{k=1}^4 (\beta_k + b_{ki}) B_k\left(\frac{t-2}{2}, \frac{\mathcal{K}-2}{2}\right) + \beta_5 \text{age}_i, \end{aligned} \quad (1)$$

where,  $m_i(t)$  denotes the measurement error free value of  $\log_2(\text{PSA} + 1)$  transformed [2, 3] measurements at time  $t$ . We model it non-linearly over time using B-splines [4]. To this end, our B-spline basis function  $B_k\{(t-2)/2, (\mathcal{K}-2)/2\}$  has 3 internal knots at  $\mathcal{K} = \{0.5, 1.3, 3\}$  years, which are the three quartiles of the observed follow-up times. The boundary knots of the spline are at 0 and 6.3 years (95-th percentile of the observed follow-up times). We mean centered (mean 2 years) and standardized (standard deviation 2 years) the follow-up time  $t$  and the knots of the B-spline  $\mathcal{K}$  during parameter estimation for better convergence. The fixed effect parameters are denoted by  $\{\beta_0, \dots, \beta_5\}$ , and  $\{b_{0i}, \dots, b_{4i}\}$  are the patient specific random effects. The random effects follow a multivariate normal distribution with mean zero and variance-covariance matrix  $\mathbf{D}$ . The error  $\varepsilon_i(t)$  is assumed to be t-distributed with three degrees of freedom (see Appendix B.1) and scale  $\sigma$ , and is independent of the random effects.

To model the impact of PSA measurements on the risk of reclassification, our joint model uses a relative risk sub-model. More specifically, the hazard of reclassification denoted as  $h_i(t)$ , and the cumulative risk of reclassification denoted as  $R_i(t)$ , at a time  $t$  are (see Panel C, Figure 1):

$$\begin{aligned} h_i(t) &= h_0(t) \exp \left( \gamma \text{age}_i + \alpha_1 m_i(t) + \alpha_2 \frac{\partial m_i(t)}{\partial t} \right), \\ R_i(t) &= \exp \left\{ - \int_0^t h_i(s) ds \right\}, \end{aligned} \quad (2)$$

where,  $\gamma$  is the parameter for the effect of age. The impact of PSA on the hazard of reclassification is modeled in two ways, namely the impact of the error free underlying PSA value  $m_i(t)$  (see Panel A, Figure 1), and the impact of the underlying PSA velocity  $\partial m_i(t)/\partial t$  (see Panel B, Figure 1).

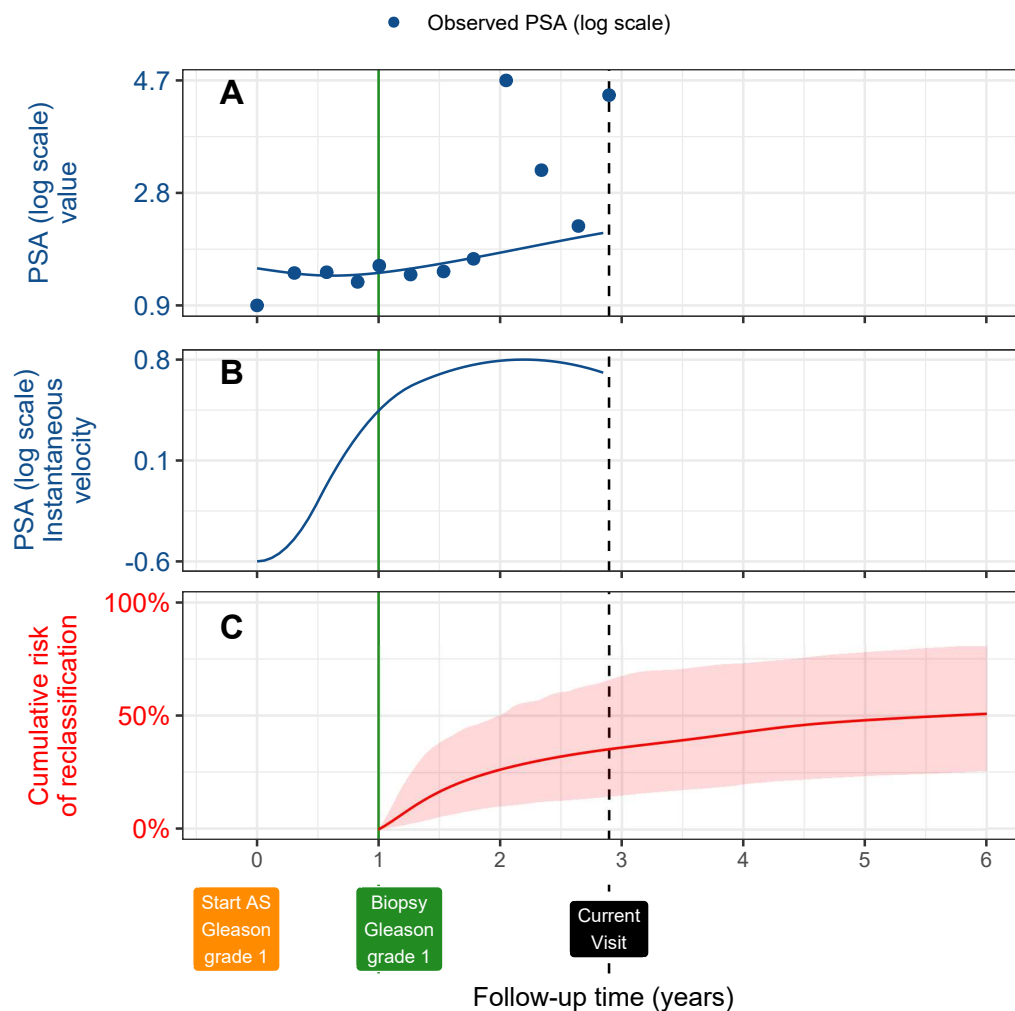


Figure 1: **Illustration of the joint model on a real PRIAS dataset patient.** **Panel A:** Observed (blue dots) and fitted PSA (solid blue line) measurements, log-transformed. **Panel B:** Estimated instantaneous velocity of PSA (log-transformed). **Panel C:** Predicted cumulative-risk of reclassification (95% credible interval shaded). Reclassification is defined as increase in Gleason grade [1] from grade 1 to 2 or higher. This risk of reclassification is available starting from the time of the latest negative biopsy (vertical green line at year 1 of follow-up). Joint model estimated it by combining the fitted PSA value and velocity (both on log scale of PSA) and time of latest negative biopsy. Black dashed line at year 4 denotes time of current visit.

The corresponding parameters are  $\alpha_1$  and  $\alpha_2$ , respectively. Lastly,  $h_0(t)$  is the baseline hazard at time  $t$ , and is modeled flexibly using P-splines [5]. More specifically:

$$\log h_0(t) = \gamma_{h_0,0} + \sum_{q=1}^Q \gamma_{h_0,q} B_q(t, \mathbf{v}),$$

where  $B_q(t, \mathbf{v})$  denotes the  $q$ -th basis function of a B-spline with knots  $\mathbf{v} = v_1, \dots, v_Q$  and vector of spline coefficients  $\gamma_{h_0}$ . To avoid choosing the number and position of knots in the spline, a relatively high number of knots (e.g., 15 to 20) are chosen and the corresponding B-spline regression coefficients  $\gamma_{h_0}$  are penalized using a differences penalty [5].

We estimate the parameters of the joint model using Markov chain Monte Carlo (MCMC) methods under the Bayesian framework. Let  $\boldsymbol{\theta}$  denote the vector of all of the parameters of the joint model. The joint model postulates that given the random effects, the time of reclassification, and the PSA measurements taken over time are all mutually independent. Under this assumption the posterior distribution of the parameters is given by:

$$\begin{aligned} p(\boldsymbol{\theta}, \mathbf{b} \mid \mathcal{D}_n) &\propto \prod_{i=1}^n p(l_i, r_i, \mathbf{y}_i \mid \mathbf{b}_i, \boldsymbol{\theta}) p(\mathbf{b}_i \mid \boldsymbol{\theta}) p(\boldsymbol{\theta}) \\ &\propto \prod_{i=1}^n p(l_i, r_i \mid \mathbf{b}_i, \boldsymbol{\theta}) p(\mathbf{y}_i \mid \mathbf{b}_i, \boldsymbol{\theta}) p(\mathbf{b}_i \mid \boldsymbol{\theta}) p(\boldsymbol{\theta}), \\ p(\mathbf{b}_i \mid \boldsymbol{\theta}) &= \frac{1}{\sqrt{(2\pi)^q \det(\mathbf{D})}} \exp(\mathbf{b}_i^T \mathbf{D}^{-1} \mathbf{b}_i), \end{aligned}$$


where, the likelihood contribution of the PSA outcome, conditional on the random effects is:

$$p(\mathbf{y}_i \mid \mathbf{b}_i, \boldsymbol{\theta}) = \frac{1}{(\sqrt{2\pi}\sigma^2)^{n_i}} \exp\left(-\frac{\|\mathbf{y}_i - \mathbf{m}_i\|^2}{\sigma^2}\right),$$

The likelihood contribution of the time of reclassification outcome is given by:

$$p(l_i, r_i \mid \mathbf{b}_i, \boldsymbol{\theta}) = \exp\left\{-\int_0^{l_i} h_i(s) ds\right\} - \exp\left\{-\int_0^{r_i} h_i(s) ds\right\}. \quad (3)$$



30 The **integral** in (3) does not have a closed-form solution, and the re we  
 31 use a 15-point Gauss-Kronrod quadrature rule to **approximate it.**

32 We use independent normal priors with zero mean and variance 100 for  
 33 the fixed effects  $\{\beta_0, \dots, \beta_5\}$ , and inverse Gamma prior with shape and rate  
 34 both equal to 0.01 for the parameter  $\sigma^2$ . For the variance-covariance matrix  
 35  $\mathbf{D}$  of the random effects we take inverse Wishart prior with an identity scale  
 36 matrix and degrees of freedom equal to 5 (number of random effects). For  
 37 the relative risk model's parameter  $\gamma$  and the association parameters  $\alpha_1, \alpha_2$ ,  
 38 we use independent normal priors with zero mean and variance 100.

#### 39 *Appendix A.1. Assumption of t-distributed (df=3) Error Terms*

40 With regards to the choice of the distribution for the error term  $\varepsilon$  for  
 41 the PSA measurements (see Equation 1), we attempted fitting multiple joint  
 42 models differing in error distribution, namely t-distribution with three, and  
 43 four degrees of freedom, and a normal distribution for the error term. How-  
 44 ever, the model assumption for the error term were best met by the model  
 45 with t-distribution having three degrees of freedom. The quantile-quantile  
 46 plot of subject-specific residuals for the corresponding model in Panel A of  
 47 Figure 2, shows that the assumption of t-distributed (df=3) errors is reason-  
 48 ably met by the fitted model.

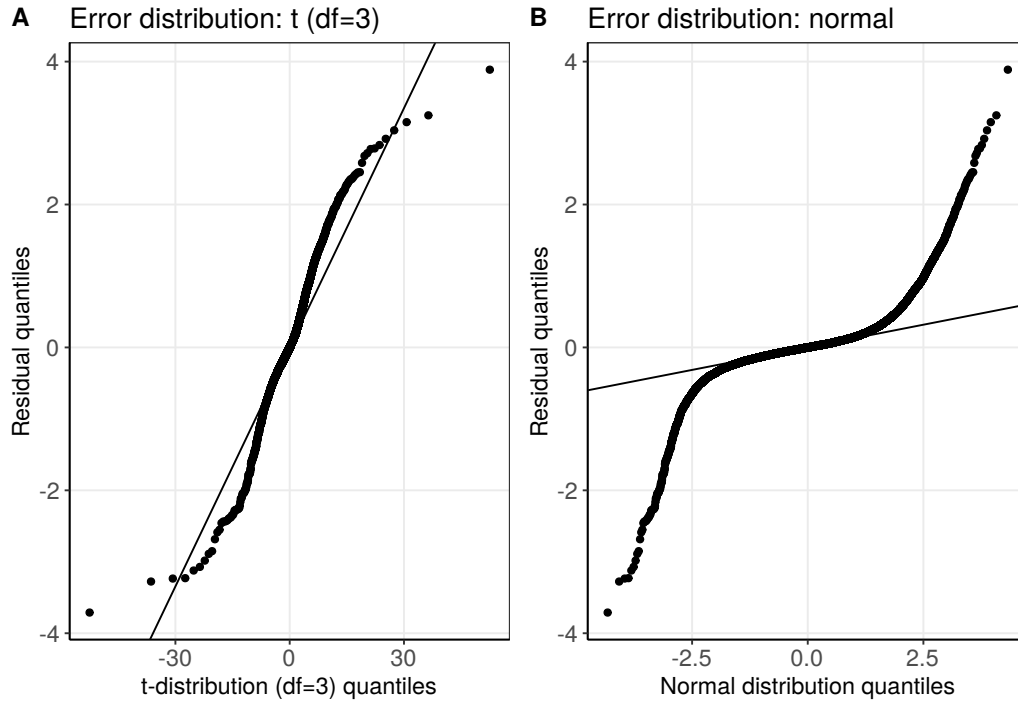


Figure 2: **Quantile-quantile plot** of subject-specific PSA residuals from two different joint models fitted to the PRIAS dataset. **Panel A:** model assuming a t-distribution ( $df=3$ ) for the error term  $\varepsilon$  (see Equation 1). **Panel B:** model assuming a normal distribution for the error term  $\varepsilon$ .

Table 1: **Estimated variance-covariance matrix  $D$**  of the random effects  $\mathbf{b} = (b_0, b_1, b_2, b_3, b_4)$  from the joint model fitted to the PRIAS dataset. The variances of the random effects are highlighted along the diagonal of the variance-covariance matrix.

Random Effects	$b_0$	$b_1$	$b_2$	$b_3$	$b_4$
$b_0$	<b>0.229</b>	0.030	0.023	0.073	0.007
$b_1$	0.030	<b>0.149</b>	0.098	0.171	0.085
$b_2$	0.023	0.098	<b>0.276</b>	0.335	0.236
$b_3$	0.073	0.171	0.335	<b>0.560</b>	0.359
$b_4$	0.007	0.085	0.236	0.359	<b>0.351</b>

Table 2: **Parameters of the longitudinal sub-model:** Estimated mean and 95% credible interval for parameters in Equation (1).

Variable	Mean	Std. Dev	2.5%	97.5%	P
Intercept	2.129	0.060	2.009	2.244	<0.001
Age	0.008	0.001	0.007	0.010	<0.001
Spline: [0.0, 0.5] years	0.063	0.007	0.051	0.075	<0.001
Spline: [0.5, 1.3] years	0.196	0.010	0.177	0.217	<0.001
Spline: [1.3, 3.0] years	0.244	0.014	0.217	0.272	<0.001
Spline: [3.0, 6.3] years	0.382	0.014	0.356	0.410	<0.001
$\sigma$	0.139	0.001	0.138	0.140	

## 49 Appendix A.2. Results

50 The joint model was fitted using the R package **JMbayes** [8]. This pack-  
 51 age utilizes the Bayesian methodology to estimate model parameters. The  
 52 corresponding posterior parameter estimates are shown in Table 2 (longitu-  
 53 dinal sub-model for PSA outcome) and Table 3 (relative risk sub-model).  
 54 The parameter estimates for the variance-covariance matrix  $D$  from the lon-  
 55 gitudinal sub-model for PSA are shown in the following Table 1:

56 For the PSA mixed effects sub-model parameter estimates (see Equa-  
 57 tion 1), in Table 2 we can see that the age of the patient trivially affects  
 58 the baseline  $\log_2(\text{PSA} + 1)$  measurement. Since the longitudinal evolution of  
 59  $\log_2(\text{PSA} + 1)$  measurements is modeled with non-linear terms, the interpre-  
 60 tation of the coefficients corresponding to time is not straightforward. In lieu  
 61 of the interpretation, in Figure 4 we present plots of observed versus fitted  
 62 PSA profiles for nine randomly selected patients.

63 For the relative risk sub-model (see Equation 2), the parameter estimates  
 64 in Table 3 show that  $\log_2(\text{PSA} + 1)$  velocity and age of the patient were  
 65 significantly associated with the hazard of reclassification.

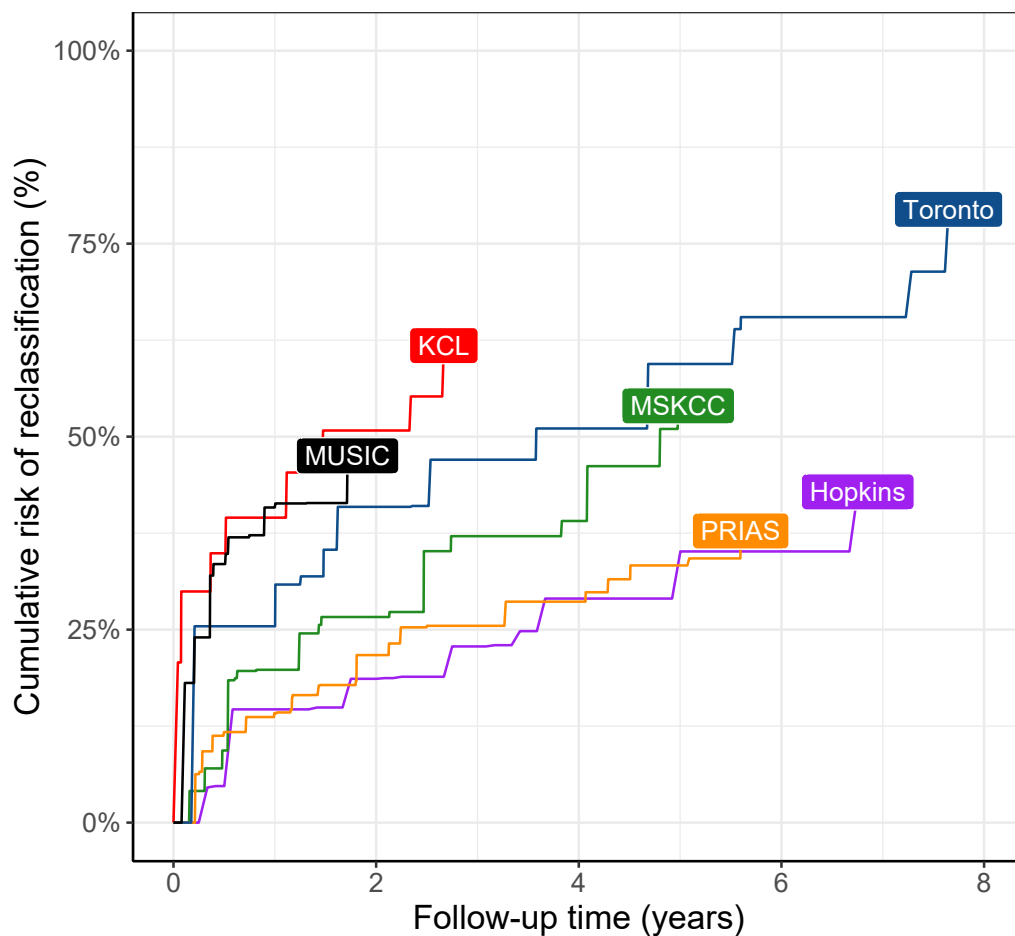


Figure 3: **Nonparametric estimate [6] of cumulative risk of reclassification** in the world's largest AS cohort PRIAS, and largest five AS cohorts from the GAP3 database [7]. Abbreviations are *Hopkins*: Johns Hopkins Active Surveillance, *PRIAS*: Prostate Cancer International Active Surveillance, *Toronto*: University of Toronto Active Surveillance, *MSKCC*: Memorial Sloan Kettering Cancer Center Active Surveillance, *KCL*: King's College London Active Surveillance, *MUSIC*: Michigan Urological Surgery Improvement Collaborative AS.



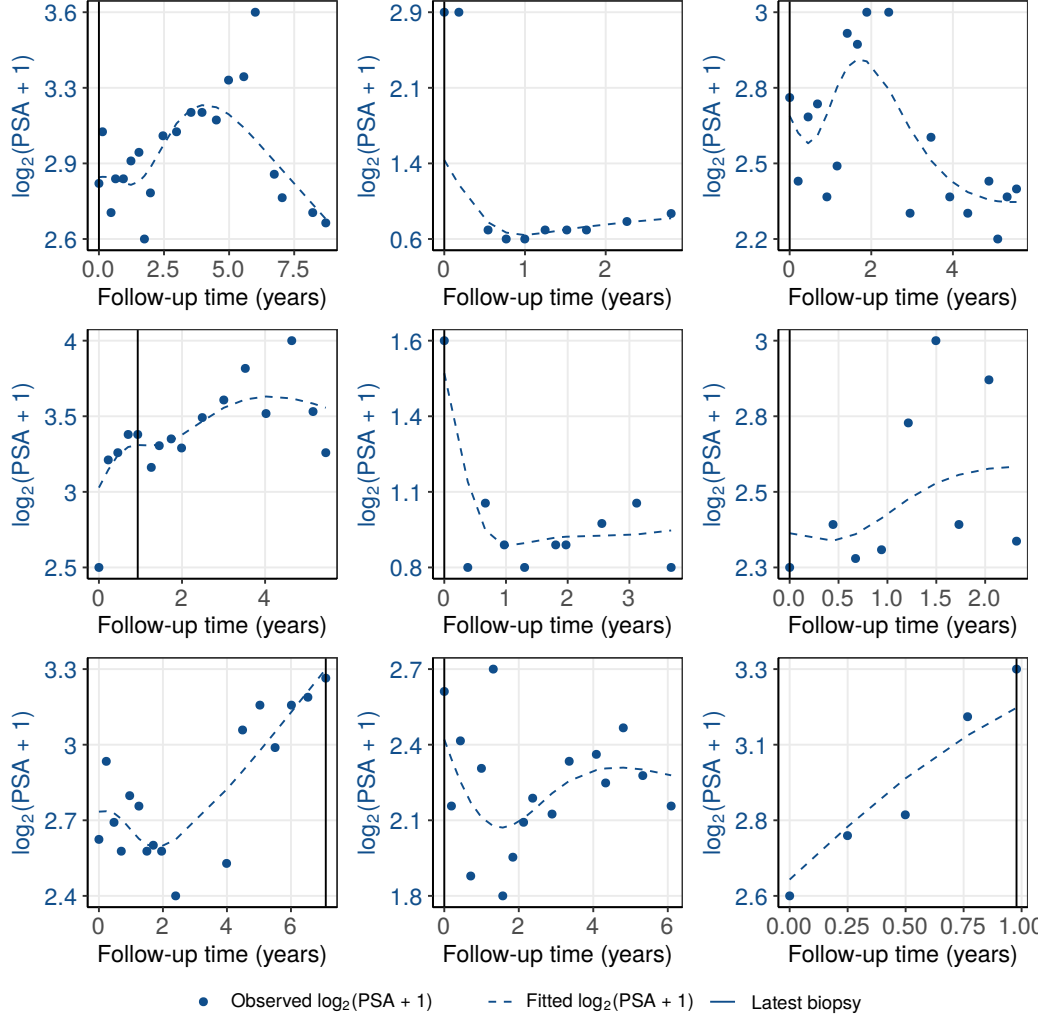


Figure 4: **Fitted versus observed  $\log_2(\text{PSA} + 1)$  profiles** for nine randomly selected PRIAS patients. The fitted profiles utilize information from the observed PSA measurements, and time of the latest biopsy.

Table 3: **Parameters of the relative risk sub-model:** Estimated mean and 95% credible interval for the parameters in Equation (2).

Variable	Mean	Std. Dev	2.5%	97.5%	P
Age	0.037	0.006	0.025	0.049	<0.001
Fitted $\log_2(\text{PSA} + 1)$ value	-0.012	0.076	-0.164	0.135	0.856
Fitted $\log_2(\text{PSA} + 1)$ velocity	2.266	0.299	1.613	2.767	<0.001

Table 4: **Hazard ratio and 95% credible interval (CI) for reclassification:** Variables are on different scale and hence we compare an increase in the variables of relative risk sub-model from their 25-th percentile ( $P_{25}$ ) to their 75-th percentile ( $P_{75}$ ). Except for age, quartiles for all other variables are based on their fitted values obtained from the joint model fitted to the PRIAS dataset.

Variable	$P_{25}$	$P_{75}$	Hazard ratio [95% CI]
Age	61	71	1.455 [1.285, 1.631]
Fitted $\log_2(\text{PSA} + 1)$ value	2.360	3.078	0.991 [0.889, 1.102]
Fitted $\log_2(\text{PSA} + 1)$ velocity	-0.085	0.308	2.433 [1.883, 2.962]

It is important to note that since age, and  $\log_2(\text{PSA} + 1)$  value and velocity are all measured on different scales, a comparison between the corresponding parameter estimates is not easy. To this end, in Table 4, we present the hazard ratio of reclassification, for an increase in the aforementioned variables from their 25-th to the 75-th percentile. For example, an increase in fitted  $\log_2(\text{PSA} + 1)$  velocity from -0.085 to 0.308 (fitted 25-th and 75-th percentiles) corresponds to a hazard ratio of 2.433. The interpretation for the rest is similar.

## 74 Appendix B. Risk Predictions for Reclassification

Let us assume a new patient  $j$ , for whom we need to estimate the risk of reclassification. Let his current follow-up visit time be  $s$ , latest time of biopsy be  $t$ , observed vector PSA measurements be  $\mathcal{Y}_j(s)$ . The combined information from the observed data about the time of reclassification, is given by the following posterior predictive distribution  $g(T_j^*)$  of his time  $T_j^*$  of reclassification:

$$\begin{aligned} g(T_j^*) &= p\{T_j^* \mid T_j^* > t, \mathcal{Y}_j(s), \mathcal{D}_n\} \\ &= \int \int p(T_j^* \mid T_j^* > t, \mathbf{b}_j, \boldsymbol{\theta}) \\ &\quad \times p\{\mathbf{b}_j \mid T_j^* > t, \mathcal{Y}_j(s), \boldsymbol{\theta}\} p(\boldsymbol{\theta} \mid \mathcal{D}_n) d\mathbf{b}_j d\boldsymbol{\theta}. \end{aligned}$$

75 The distribution  $g(T_j^*)$  depends not only depends on the observed data of the  
 76 patient  $T_j^* > t, \mathcal{Y}_j(s)$ , but also depends on the information from the PRIAS  
 77 dataset  $\mathcal{D}_n$ . To this the the posterior distribution of random effects  $\mathbf{b}_j$  and  
 78 posterior distribution of the vector of all parameters  $\boldsymbol{\theta}$  are utilized, respec-  
 79 tively. The distribution  $g(T_j^*)$  can be estimated as detailed in Rizopoulos  
 80 et al. [9]. Since, majority of the prostate cancer patients may not obtain  
 81 reclassification in the current follow-up period of PRIAS (thirteen years),  
 82  $g(T_j^*)$  can only be estimated for a limited follow-up period.

The cumulative risk of reclassification can be derived from  $g(T_j^*)$  as given in [9]. It is given by:

$$R_j(u \mid t, s) = \Pr\{T_j^* > u \mid T_j^* > t, \mathcal{Y}_j(s), \mathcal{D}_n\}, \quad u \geq t. \quad (4)$$

83 The personalized risk profile of the patient (see Panel C, Figure 5) updates  
 84 as more data is gathered over follow-up visits.

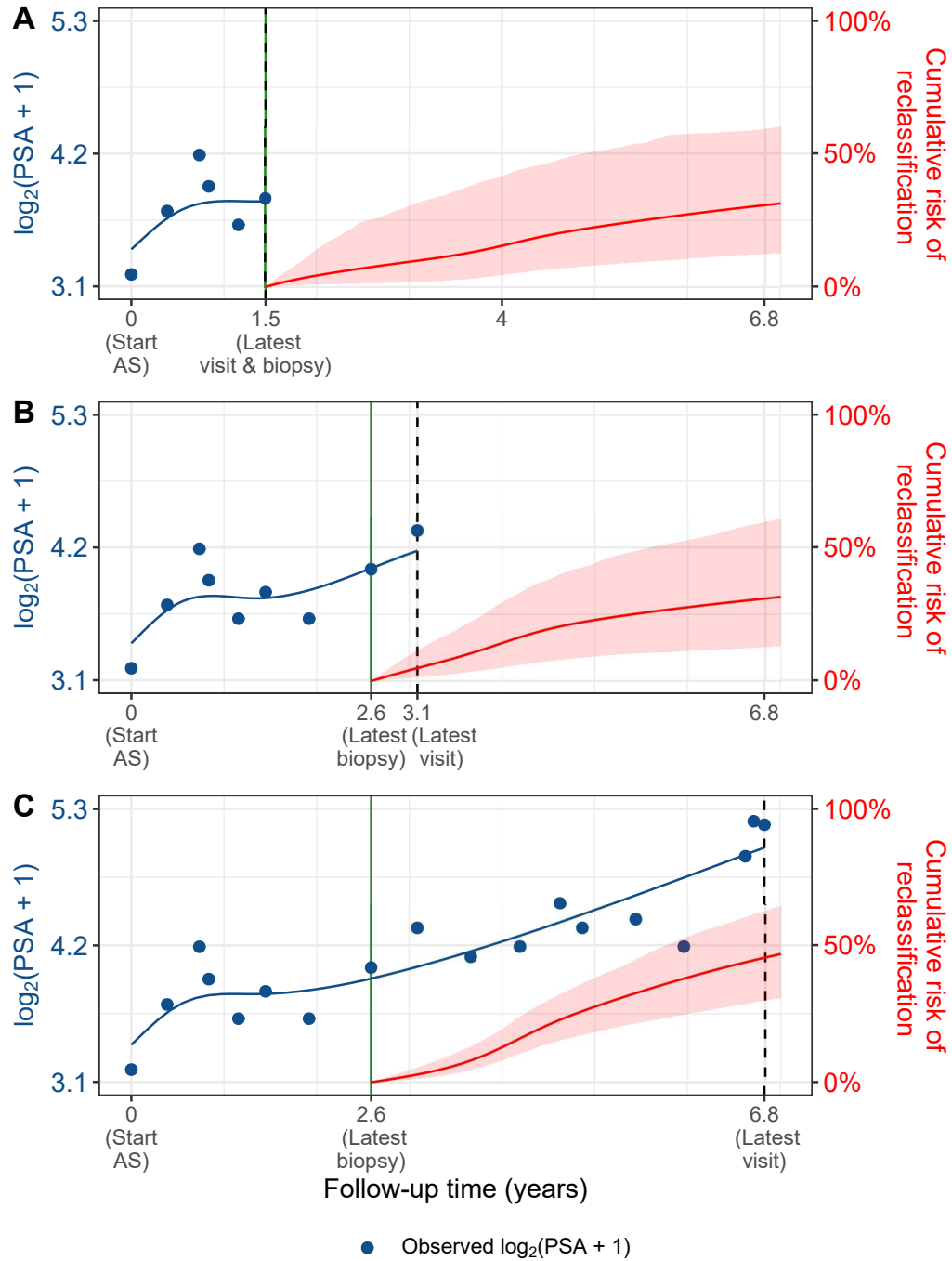


Figure 5: **Cumulative risk of (reclassification) changing dynamically over follow-up** as more patient data is gathered. The three **Panels A,B and C**: are ordered by the time of the latest visit (dashed vertical black line) of a new patient. At each of the latest follow-up visits, we combine the accumulated PSA measurements (shown in blue), and latest time of negative biopsy (solid vertical green line) to obtain the updated cumulative risk profile (shown in red) of the patient.

85 *Appendix B.1. Validation of Risk Predictions*

86 We wanted to check the usefulness of our model for not only the PRIAS  
 87 patients but also for patients from other cohorts. To this end, we validated  
 88 our model in the PRIAS dataset (internal validation) and in largest five co-  
 89 horts from the GAP3 database [7]. These are the University of Toronto AS  
 90 (Toronto), Johns Hopkins AS (Hopkins), Memorial Sloan Kettering Cancer  
 91 Center AS (MSKCC), King’s College London AS (KCL), and Michigan Uro-  
 92 logical Surgery Improvement Collaborative AS (MUSIC).

**Calibration-in-the-large** We first assessed calibration-in-the-large [10]  
 of our model in the aforementioned cohorts. To this end, we used our model  
 to predict the cumulative risk of reclassification for each patient given their  
 PSA measurements and biopsy results. We then averaged the resulting pro-  
 files of cumulative risk of reclassification. Subsequently we compared the  
 averaged cumulative-risk profile with a non-parametric estimate [6] of the  
 cumulative risk of reclassification in each of the cohorts. The results are  
 shown in Panel A of Figure 6. We can see that our model’s calibration is fine  
 only in PRIAS and Hopkins cohorts. To improve our model’s calibration in  
 KCL, MUSIC, Toronto, and MSKCC cohorts, we recalibrated the baseline  
 hazard of the joint model fitted to the PRIAS dataset, individually for each  
 of these cohorts. More specifically, given the data of an external cohort  $\mathcal{D}_n^c$ ,  
 where  $c$  denotes the cohort, the recalibrated parameters  $\gamma_{h0}^c$  (Appendix A)  
 of the log baseline hazard are given by:

$$p(\gamma_{h0}^c \mid \mathcal{D}_n^c, \mathbf{b}^c, \boldsymbol{\theta}) \propto \prod_{i=1}^{n^c} p(l_i^c, r_i^c \mid \mathbf{b}_i^c, \boldsymbol{\theta}) p(\gamma_{h0}^c) \quad (5)$$

93 where  $n^c$  are the number of patients in the  $c$ -th cohort and  $\boldsymbol{\theta}$  are the pa-  
 94 rameters of the joint model fitted to the PRIAS dataset. The interval in  
 95 which reclassification is observed for the  $i$  – th patient is given by  $l_i^c, r_i^c$ , with  
 96  $r_i^c = \infty$  for right censored patients. The symbol  $\mathbf{b}_i^c$  denotes patient-specific  
 97 random effects (Appendix A). The random effects are obtained using the joint  
 98 model fitted to the PRIAS dataset prior to recalibration. We re-evaluated the  
 99 calibration-in-the-large of our model after the recalibration of the baseline  
 100 hazard individually for each cohort. The improved calibration-in-the-large is  
 101 shown in Panel B of Figure 6.

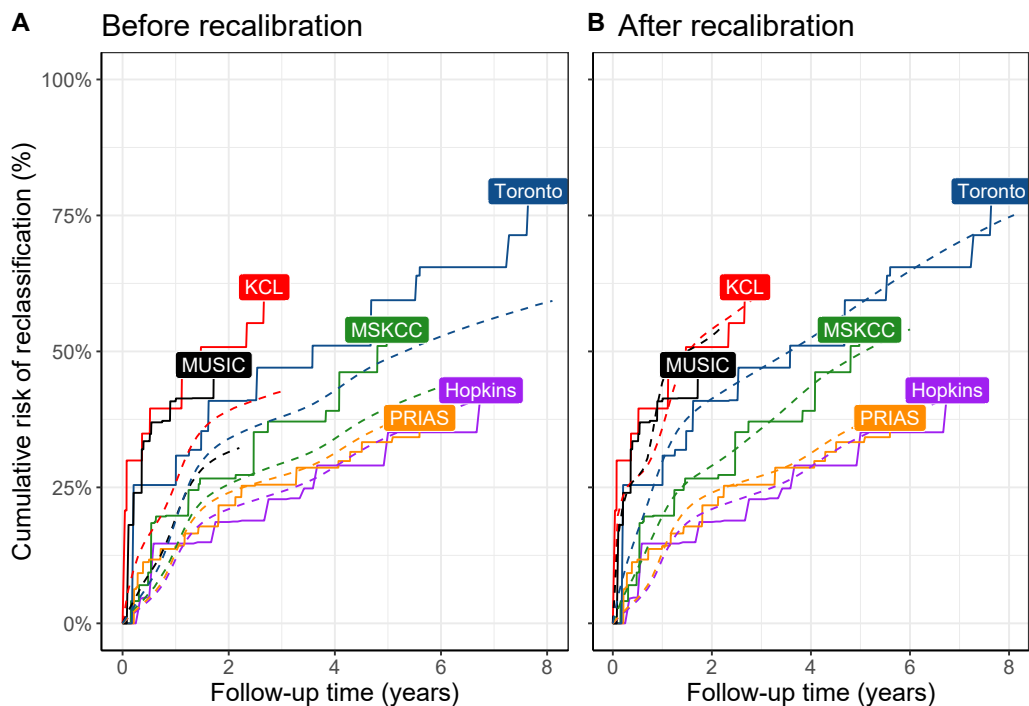


Figure 6: **Calibration-in-the-large of our model:** In **Panel A** we can see that our model is not well calibrated for use in KCL, MUSIC, Toronto and MSKCC. In **Panel B** we can see that calibration of model predictions improved in KCL, MUSIC, Toronto and MSKCC cohorts after recalibrating our model. Recalibration was not necessary for Hopkins cohort. Full names of Cohorts are *PRIAS*: Prostate Cancer International Active Surveillance, *Toronto*: University of Toronto Active Surveillance, *Hopkins*: Johns Hopkins Active Surveillance, *MSKCC*: Memorial Sloan Kettering Cancer Center Active Surveillance, *KCL*: King's College London Active Surveillance, *MUSIC*: Michigan Urological Surgery Improvement Collaborative Active Surveillance.

102 **Recalibrated PRIAS Model Versus Individual Joint Models**  
 103 **For Each Cohort** We wanted to check if our recalibrated PRIAS model  
 104 performed as good as a new joint model that could be fitted to the external  
 105 cohorts. To this end, we predicted cumulative-risk of reclassification for each  
 106 patient from each cohort using two different models, namely the recalibrated  
 107 PRIAS model for that cohort, and a new joint model fitted to that cohort.  
 108 The difference in predicted cumulative-risk of reclassification from these co-  
 109 horts (Figure 7) is quite small. The only exception is the MUSIC cohort  
 110 in which individual risk predictions obtained from the recalibrated PRIAS  
 111 model may differ from predictions from a newly fitted joint model, by more  
 112 than 10% in at least half of the patients.

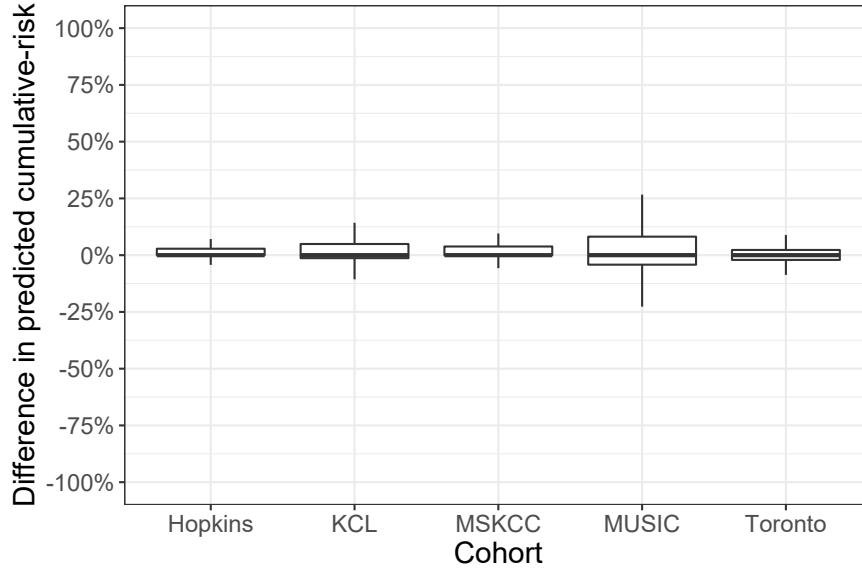


Figure 7: **Comparison of predictions from recalibrated PRIAS model with individual joint models fitted to external cohorts:** On Y-axis we show the difference between predicted cumulative-risk of reclassification for individual patients using two models, namely the recalibrated PRIAS model for each cohort, and individual joint model fitted to each cohort. The maximum differences in each direction can be 100% or -100%. The figure shows that in all cohorts except the MUSIC cohort, the recalibrated PRIAS model predicts as good as a newly fitted joint model to each of the cohorts. Full names of Cohorts are *PRIAS*: Prostate Cancer International Active Surveillance, *Toronto*: University of Toronto Active Surveillance, *Hopkins*: Johns Hopkins Active Surveillance, *MSKCC*: Memorial Sloan Kettering Cancer Center Active Surveillance, *KCL*: King’s College London Active Surveillance, *MUSIC*: Michigan Urological Surgery Improvement Collaborative Active Surveillance.

**Validation of Dynamic Cumulative-Risk Predictions** As shown in Figure 5 the cumulative-risk predictions from the joint model are dynamic in nature. That is, they update as more data becomes available over time. Consequently, the discrimination and calibration of the joint model also depends on the available data. We assessed these two measures dynamically in the PRIAS cohort (interval validation) and in the largest five external cohorts that are part of the GAP3 database. For discrimination we utilized the time-varying area under the receiver operating characteristic curve or time-varying AUC [9]. For time-varying calibration we assessed the mean absolute prediction error or MAPE [9]. The AUC indicates how well the model discriminates between patients who experience reclassification and those do not. The MAPE indicates how accurately the model predicts reclassification. Both AUC and MAPE are restricted to  $[0, 1]$ . However, it is preferred that  $\text{AUC} > 0.5$  because an  $\text{AUC} \leq 0.5$  indicates that the model performs worse than random discrimination. Ideally MAPE should be 0.

We calculate AUC and MAPE in a time-dependent manner. More specifically, given the time of latest biopsy  $t$ , and history of PSA measurements up to time  $s$ , we calculate AUC and MAPE for a medically relevant time frame  $(t, s]$ , within which the occurrence of reclassification is of interest. In the case of prostate cancer, at any point in time  $s$  it is of interest to identify patients who may have experienced reclassification in the last one year  $(s - 1, s]$ . That is we set  $t = s - 1$ . We then calculate AUC and MAPE at a gap of every six months (follow-up schedule of PRIAS). That is,  $s \in \{1, 1.5, \dots\}$  years. To obtain reliable estimates of AUC and MAPE, in each cohort we restrict  $s$  to a maximum time point  $s_{\max}$ , such that there are at least 10 patients who experience reclassification after  $s_{\max}$ . This maximum time point  $s_{\max}$  differs between cohorts, and is given in Table 5.

The results for estimates of AUC and MAPE are summarized in Figure 8, and in Table 6 to Table 11. Results are based on the recalibrated PRIAS model for Toronto, MSKCC, MUSIC, and KCL cohorts, whereas original joint model fitted to the PRIAS dataset is used for Hopkins and PRIAS cohorts. The results show that AUC remains more or less constant in all cohorts as more data becomes available for patients. The AUC obtains a moderate value, roughly between 0.5 and 0.7 for all cohorts. On the other hand, MAPE reduces by a big margin after year two of follow-up. This could be because of two reasons. Firstly, MAPE at year one is based only on four PSA measurements gathered in first year of follow-up, whereas after year two number of PSA measurements increase. Secondly, patients in year one consist



Table 5: **Maximum follow-up period up to which we can reliably predict risk of reclassification.** In each cohort, this time point is chosen such that there are at least 10 patients who experience reclassification after this time point. Full names of Cohorts are *PRIAS*: Prostate Cancer International Active Surveillance, *Toronto*: University of Toronto Active Surveillance, *Hopkins*: Johns Hopkins Active Surveillance, *MSKCC*: Memorial Sloan Kettering Cancer Center Active Surveillance, *KCL*: King's College London Active Surveillance, *MUSIC*: Michigan Urological Surgery Improvement Collaborative Active Surveillance.

Cohort	Maximum Prediction Time (years)
PRIAS	6
KCL	3
MUSIC	2
Toronto	8
MSKCC	6
Hopkins	7



151 of two sub-populations, namely patients with a correct Gleason grade 1 at the  
 152 time of inclusion in AS, and patients who probably had Gleason grade 2 at  
 153 inclusion but were misclassified by the urologist as Gleason grade 1 patients.  
 154 To remedy this problem, a biopsy for all patients at year one is commonly  
 155 recommended in all AS programs [11].

Table 6: **Internal validation of predictions of reclassification in PRIAS cohort.** The area under the receiver operating characteristic curve or AUC (measure of discrimination) and mean absolute prediction error or MAPE (measure of calibration) are calculated over the follow-up period at a gap of 6 months. In addition bootstrapped 95% confidence intervals (CI) are also presented.

Follow-up period (years)	AUC (95% CI)	MAPE (95%CI)
0.0 to 1.0	0.652 [0.611, 0.690]	0.220 [0.214, 0.227]
0.5 to 1.5	0.657 [0.641, 0.673]	0.260 [0.254, 0.265]
1.0 to 2.0	0.661 [0.647, 0.678]	0.187 [0.183, 0.191]
1.5 to 2.5	0.647 [0.596, 0.688]	0.129 [0.122, 0.140]
2.0 to 3.0	0.683 [0.642, 0.723]	0.135 [0.125, 0.146]
2.5 to 3.5	0.692 [0.632, 0.748]	0.118 [0.111, 0.128]
3.0 to 4.0	0.657 [0.603, 0.709]	0.086 [0.080, 0.092]
3.5 to 4.5	0.623 [0.582, 0.660]	0.111 [0.105, 0.116]
4.0 to 5.0	0.619 [0.582, 0.654]	0.126 [0.118, 0.131]
4.5 to 5.5	0.624 [0.537, 0.711]	0.119 [0.103, 0.135]
5.0 to 6.0	0.639 [0.582, 0.696]	0.121 [0.103, 0.138]

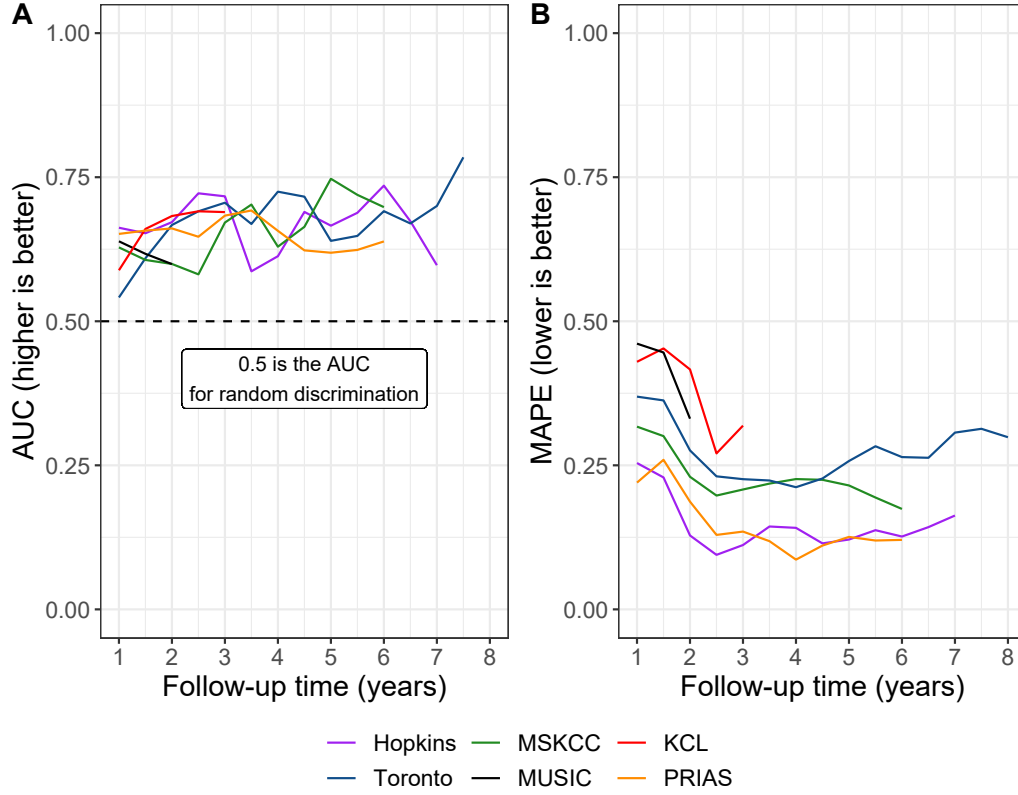


**Figure 8: Validation of Dynamic Cumulative-Risk Predictions.** In **Panel A** we can see that the time dependent area under the receiver operating characteristic curve or AUC (measure of discrimination) is above 0.5 in PRIAS (internal validation), and in Toronto, Hopkins, MSKCC, KCL, and MUSIC AS cohorts (external validation). In **Panel B** we can see that the time dependent root mean squared prediction error or MAPE (measure of calibration) is similar for PRIAS, and Hopkins and Toronto cohorts. The bootstrapped 95% confidence interval for these estimates are presented in Table 6 to Table 10. Full names of Cohorts are *PRIAS*: Prostate Cancer International Active Surveillance, *Toronto*: University of Toronto Active Surveillance, *Hopkins*: Johns Hopkins Active Surveillance, *MSKCC*: Memorial Sloan Kettering Cancer Center Active Surveillance, *KCL*: King's College London Active Surveillance, *MUSIC*: Michigan Urological Surgery Improvement Collaborative Active Surveillance.

Table 7: **External validation of predictions of reclassification in University of Toronto Active Surveillance cohort.** The area under the receiver operating characteristic curve or AUC (measure of discrimination) and mean absolute prediction error or MAPE (measure of calibration) are calculated over the follow-up period at a gap of 6 months. In addition bootstrapped 95% confidence intervals (CI) are also presented.

Follow-up period (years)	AUC (95% CI)	MAPE (95%CI)
0.0 to 1.0	0.541 [0.470, 0.621]	0.369 [0.352, 0.381]
0.5 to 1.5	0.609 [0.547, 0.661]	0.363 [0.348, 0.376]
1.0 to 2.0	0.667 [0.634, 0.712]	0.276 [0.259, 0.296]
1.5 to 2.5	0.691 [0.651, 0.730]	0.231 [0.205, 0.254]
2.0 to 3.0	0.706 [0.637, 0.762]	0.226 [0.196, 0.260]
2.5 to 3.5	0.669 [0.586, 0.741]	0.224 [0.195, 0.258]
3.0 to 4.0	0.725 [0.649, 0.806]	0.212 [0.184, 0.238]
3.5 to 4.5	0.716 [0.642, 0.793]	0.227 [0.206, 0.258]
4.0 to 5.0	0.640 [0.579, 0.717]	0.257 [0.222, 0.312]
4.5 to 5.5	0.648 [0.579, 0.740]	0.283 [0.247, 0.326]
5.0 to 6.0	0.691 [0.608, 0.793]	0.264 [0.232, 0.302]
5.5 to 6.5	0.670 [0.543, 0.776]	0.263 [0.227, 0.307]
6.0 to 7.0	0.700 [0.544, 0.851]	0.307 [0.258, 0.363]
6.5 to 7.5	0.785 [0.640, 0.866]	0.313 [0.272, 0.360]
7.0 to 8.0	0.688 [0.532, 0.786]	0.299 [0.249, 0.361]

Table 8: **External validation of predictions of reclassification in Johns Hopkins Active Surveillance cohort.** The area under the receiver operating characteristic curve or AUC (measure of discrimination) and mean absolute prediction error or MAPE (measure of calibration) are calculated over the follow-up period at a gap of 6 months. In addition bootstrapped 95% confidence intervals (CI) are also presented.

Follow-up period (years)	AUC (95% CI)	MAPE (95%CI)
0.0 to 1.0	0.662 [0.586, 0.715]	0.254 [0.245, 0.265]
0.5 to 1.5	0.653 [0.603, 0.707]	0.229 [0.219, 0.240]
1.0 to 2.0	0.672 [0.604, 0.744]	0.128 [0.115, 0.141]
1.5 to 2.5	0.722 [0.652, 0.792]	0.095 [0.081, 0.111]
2.0 to 3.0	0.717 [0.638, 0.777]	0.112 [0.100, 0.123]
2.5 to 3.5	0.587 [0.493, 0.704]	0.144 [0.129, 0.154]
3.0 to 4.0	0.613 [0.486, 0.742]	0.141 [0.126, 0.156]
3.5 to 4.5	0.690 [0.594, 0.783]	0.115 [0.100, 0.133]
4.0 to 5.0	0.666 [0.572, 0.754]	0.121 [0.104, 0.147]
4.5 to 5.5	0.688 [0.519, 0.779]	0.137 [0.119, 0.161]
5.0 to 6.0	0.735 [0.676, 0.820]	0.126 [0.102, 0.152]
5.5 to 6.5	0.674 [0.581, 0.765]	0.143 [0.121, 0.172]
6.0 to 7.0	0.597 [0.472, 0.712]	0.163 [0.126, 0.195]

Table 9: **External validation of predictions of reclassification in Memorial Sloan Kettering Cancer Center Active Surveillance cohort.** The area under the receiver operating characteristic curve or AUC (measure of discrimination) and mean absolute prediction error or MAPE (measure of calibration) are calculated over the follow-up period at a gap of 6 months. In addition bootstrapped 95% confidence intervals (CI) are also presented.

Follow-up period (years)	AUC (95% CI)	MAPE (95%CI)
0.0 to 1.0	0.628 [0.577, 0.688]	0.317 [0.316, 0.318]
0.5 to 1.5	0.606 [0.532, 0.657]	0.301 [0.290, 0.311]
1.0 to 2.0	0.599 [0.518, 0.671]	0.230 [0.207, 0.256]
1.5 to 2.5	0.581 [0.504, 0.663]	0.198 [0.168, 0.235]
2.0 to 3.0	0.671 [0.599, 0.741]	0.208 [0.182, 0.232]
2.5 to 3.5	0.703 [0.610, 0.777]	0.218 [0.197, 0.246]
3.0 to 4.0	0.629 [0.499, 0.706]	0.226 [0.194, 0.259]
3.5 to 4.5	0.664 [0.589, 0.756]	0.225 [0.199, 0.262]
4.0 to 5.0	0.747 [0.642, 0.841]	0.215 [0.188, 0.247]
4.5 to 5.5	0.719 [0.597, 0.852]	0.194 [0.165, 0.232]
5.0 to 6.0	0.698 [0.565, 0.792]	0.174 [0.136, 0.227]

Table 10: **External validation of predictions of reclassification in King's College London Active Surveillance cohort.** The area under the receiver operating characteristic curve or AUC (measure of discrimination) and mean absolute prediction error or MAPE (measure of calibration) are calculated over the follow-up period at a gap of 6 months. In addition bootstrapped 95% confidence intervals (CI) are also presented.

Follow-up period (years)	AUC (95% CI)	MAPE (95%CI)
0.0 to 1.0	0.589 [0.514, 0.653]	0.430 [0.407, 0.450]
0.5 to 1.5	0.660 [0.550, 0.742]	0.453 [0.431, 0.474]
1.0 to 2.0	0.683 [0.604, 0.753]	0.416 [0.396, 0.445]
1.5 to 2.5	0.691 [0.621, 0.766]	0.271 [0.246, 0.297]
2.0 to 3.0	0.689 [0.616, 0.785]	0.319 [0.282, 0.344]

Table 11: **External validation of predictions of reclassification in Michigan Urological Surgery Improvement Collaborative Active Surveillance cohort.** The area under the receiver operating characteristic curve or AUC (measure of discrimination) and mean absolute prediction error or MAPE (measure of calibration) are calculated over the follow-up period at a gap of 6 months. In addition bootstrapped 95% confidence intervals (CI) are also presented.

Follow-up period (years)	AUC (95% CI)	MAPE (95%CI)
0.0 to 1.0	0.639 [0.607, 0.672]	0.461 [0.450, 0.469]
0.5 to 1.5	0.617 [0.588, 0.652]	0.446 [0.441, 0.453]
1.0 to 2.0	0.599 [0.553, 0.632]	0.331 [0.317, 0.348]

## 156 Appendix C. Personalized Biopsies Based on Risk of Reclassifica- 157 tion

158 Consider some real patients from the PRIAS database shown in Figure 9  
159 to Figure 11. We intend to develop personalized schedule of biopsies for these  
160 patients. Using the joint model fitted to the PRIAS dataset, we first obtain  
161 their cumulative risk of reclassification over the entire follow-up period (see  
162 Equation 4, given their accumulated clinical data. Assume a new patient  $j$   
163 whose latest biopsy was conducted at time  $t$  and who has visited the clinic  
164 at the current time  $s$ . We suggest a biopsy at his current visit time  $s$  if  
165 his cumulative risk of reclassification at  $s$  given by  $R_j(s | t)$  (Appendix  
166 B) is above a certain threshold (e.g., 10% risk). As an example, let us  
167 assume that using this rule we decide to schedule a biopsy at time  $s$ . Since  
168 this patient may be removed from AS upon detection of reclassification, the  
169 schedule of remaining future biopsies can only be made under the assumption  
170 that reclassification could not be observed at  $s$ . Under this assumption we  
171 update the patient’s cumulative risk of reclassification at next visit time  
172  $s + 1$  to be  $R_j(s + 1 | s)$ . Now, if  $R_j(s + 1 | s) < 10\%$ , then we will  
173 not schedule a biopsy at  $s + 1$ . Instead, we will decide for a biopsy at a  
174 subsequent time  $s + 2$  using the cumulative risk  $R_j(s + 2 | s)$ . If however,  
175 at time  $s + 1$  the cumulative risk of reclassification  $R_j(s + 1 | s) \geq 10\%$   
176 then we would have decided for a biopsy at  $s + 1$ . Consequently, the biopsy  
177 decision at time  $s + 2$  would have been made using the updated cumulative  
178 risk  $R_j(s + 2 | s + 1)$  and not  $R_j(s + 2 | s)$ . We repeat this process for a  
179 fixed horizon in each cohort (PRIAS and five external GAP3 cohorts). This  
180 horizon is the maximum time point  $t_h$ , such that there are at least 10 patients  
181 who experience reclassification after  $t_h$  (Table 12). This horizon is six years  
182 in PRIAS. While scheduling these biopsies we always maintain a minimum  
183 gap of one year, as recommended in PRIAS. Personalized schedules can also  
184 be made with any other risk threshold such as 5% or 15%.

To assist patients in making an informed choice for a schedule, be it per-  
sonalized or fixed, we provide them patient-specific consequences of following  
each schedule. To this end, we first calculate the probability of occurrence  
of reclassification between successive biopsies of each schedule. Using these  
probabilities we then obtain the expected delay in detection of reclassifica-  
tion for following that schedule. Thus, patients have a method to compare  
across various schedules in terms of the personalized burden (time and total  
biopsies), and personalized benefit (less delay in detection of reclassification

Table 12: **Maximum follow-up period up to which we can reliably make personalized schedules.** In each cohort, this time point is chosen such that there are at least 10 patients who experience reclassification after this time point. Full names of Cohorts are *PRIAS*: Prostate Cancer International Active Surveillance, *Toronto*: University of Toronto Active Surveillance, *Hopkins*: Johns Hopkins Active Surveillance, *MSKCC*: Memorial Sloan Kettering Cancer Center Active Surveillance, *KCL*: King's College London Active Surveillance, *MUSIC*: Michigan Urological Surgery Improvement Collaborative Active Surveillance.

Cohort	Maximum Personalized Schedule Time (years)
PRIAS	6
KCL	3
MUSIC	2
Toronto	8
MSKCC	6
Hopkins	7

is beneficial). Suppose once again that for patient  $j$ , the time of latest negative biopsy is  $t_0$ , and current visit time is  $s > t_0$ . Then equation for the expected delay  $D_j(\mathcal{S} \mid t, s)$  in detection of reclassification using schedule of biopsies  $\mathcal{S} = \{t_1, \dots, t_h\}$ , where  $t_1 \geq s$ , and  $t_h$  is the horizon time up to which we want to schedule biopsies, is given by:

$$D_j(\mathcal{S} \mid t, s) = \sum_{v=1}^h R_j(t_v \mid t_{v-1}, s) \times \left\{ t_v - t_{v-1} - \int_{t_{v-1}}^{t_v} S_j(u \mid t_v, t_{v-1}, s) du \right\},$$

$$S_j(u \mid t_v, t_{v-1}, s) = \Pr\{T_j^* > u \mid t_v \geq T_j^* > t_{v-1}, \mathcal{Y}_j(s), \mathcal{D}_n\}, \quad t_v \geq u > t_{v-1}, \quad (6)$$

185 and  $R_j(t_v \mid t_{v-1}, s)$  is as defined in Equation (4). The personalized and fixed  
 186 schedules, and their consequences for a few real patients from the PRIAS  
 187 dataset are shown in Figure 9 to Figure 11. A compulsory biopsy was done  
 188 at horizon  $t_h$  of follow-up in all schedules for meaningful comparison of their  
 189 expected delays in detection of reclassification.

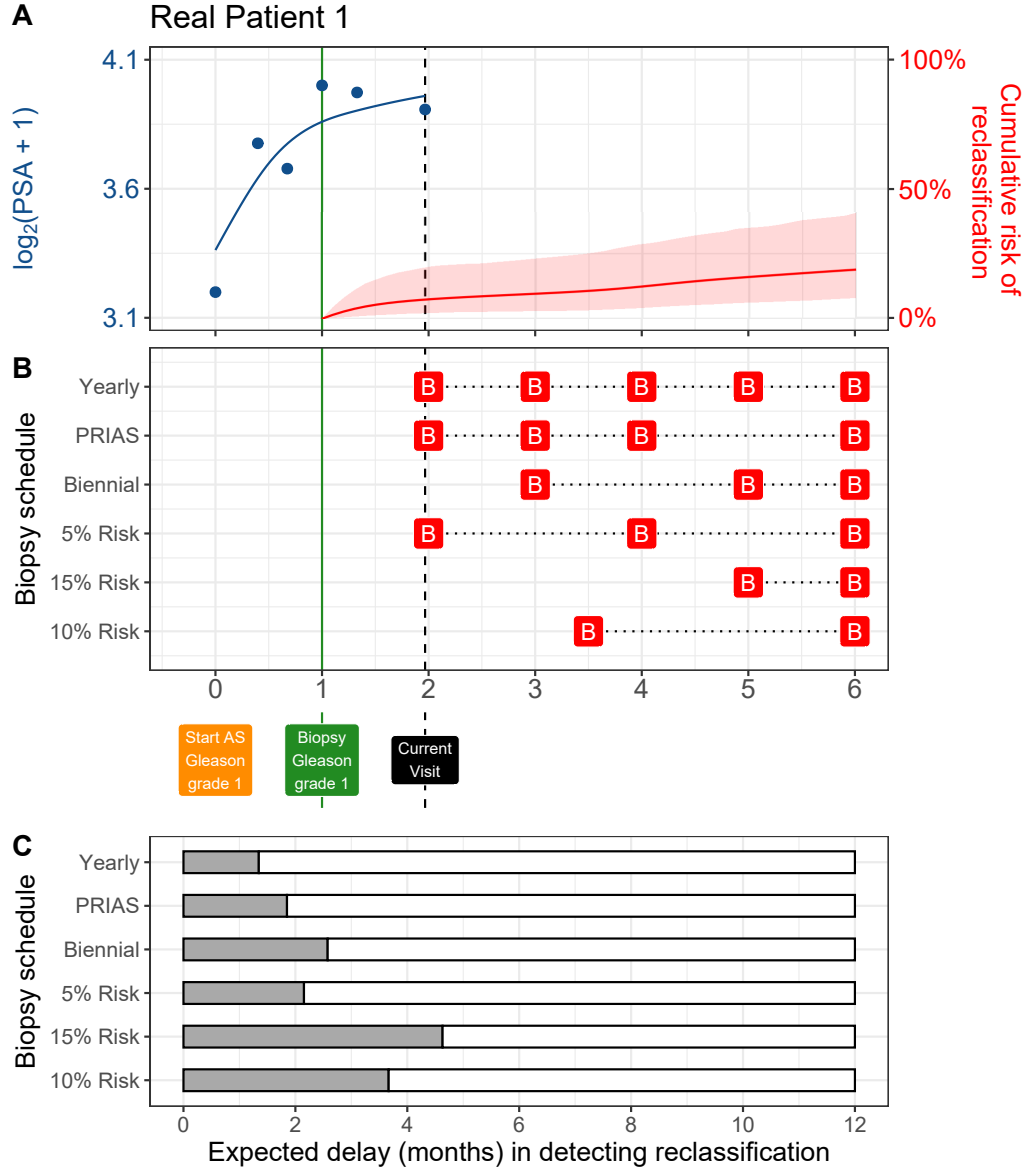


Figure 9: **Personalized and fixed schedules of biopsies for patient 1.** **Panel A:** shows the observed and fitted  $\log_2(\text{PSA} + 1)$  measurements (Equation 1), and the dynamic cumulative risk of reclassification (see Appendix B) over follow-up period. **Panel B** shows the personalized and fixed schedules of biopsies with a 'B' indicating times of biopsies. **Panel C** various schedules are compared in terms of the expected delay in detection of reclassification if they are followed.



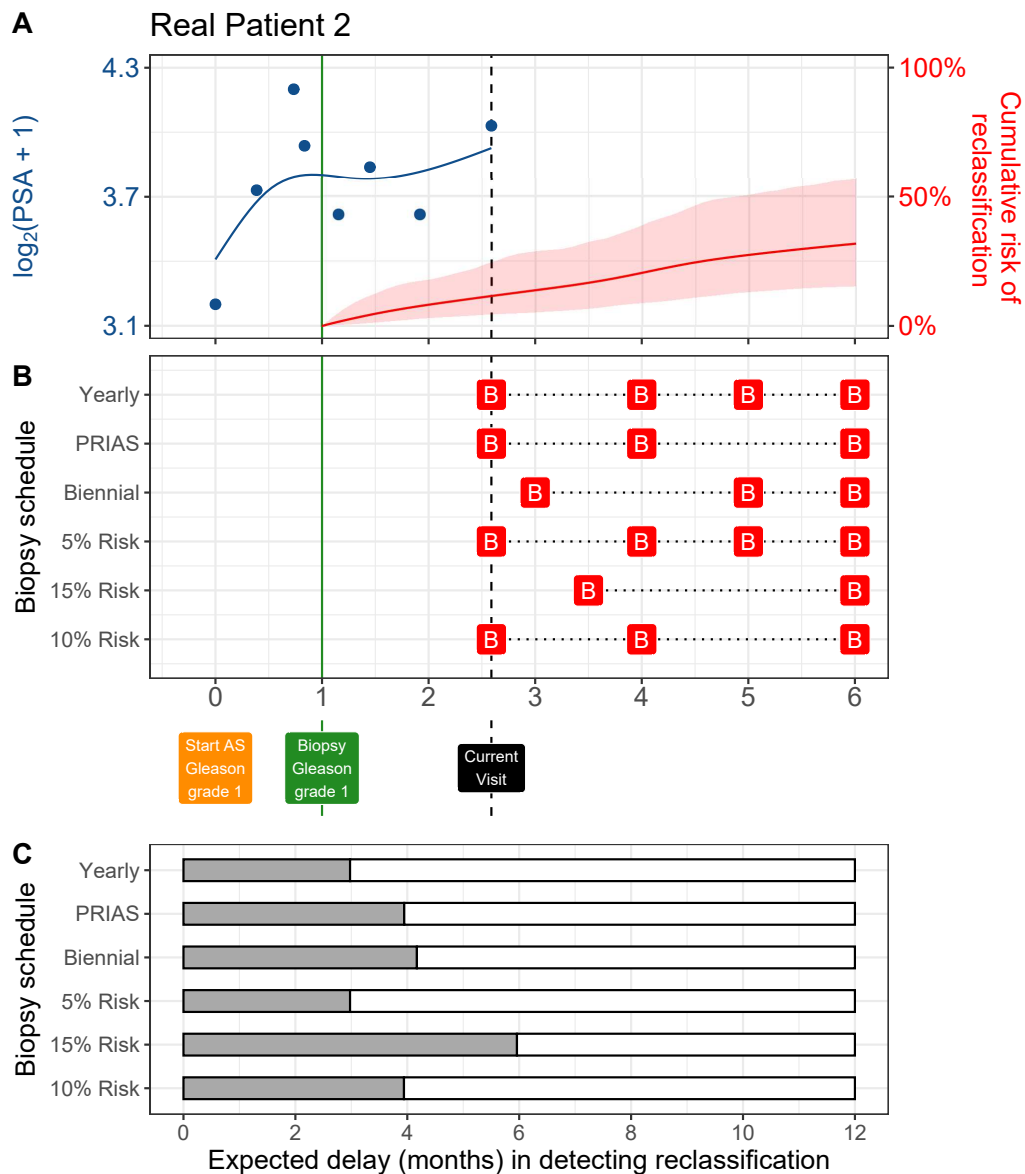


Figure 10: **Personalized and fixed schedules of biopsies for patient 2.** **Panel A:** shows the observed and fitted  $\log_2(\text{PSA} + 1)$  measurements (Equation 1), and the dynamic cumulative risk of reclassification (see Appendix B) over follow-up period. **Panel B** shows the personalized and fixed schedules of biopsies with a 'B' indicating times of biopsies. **Panel C** compares various schedules in terms of the expected delay in detection of reclassification if they are followed.

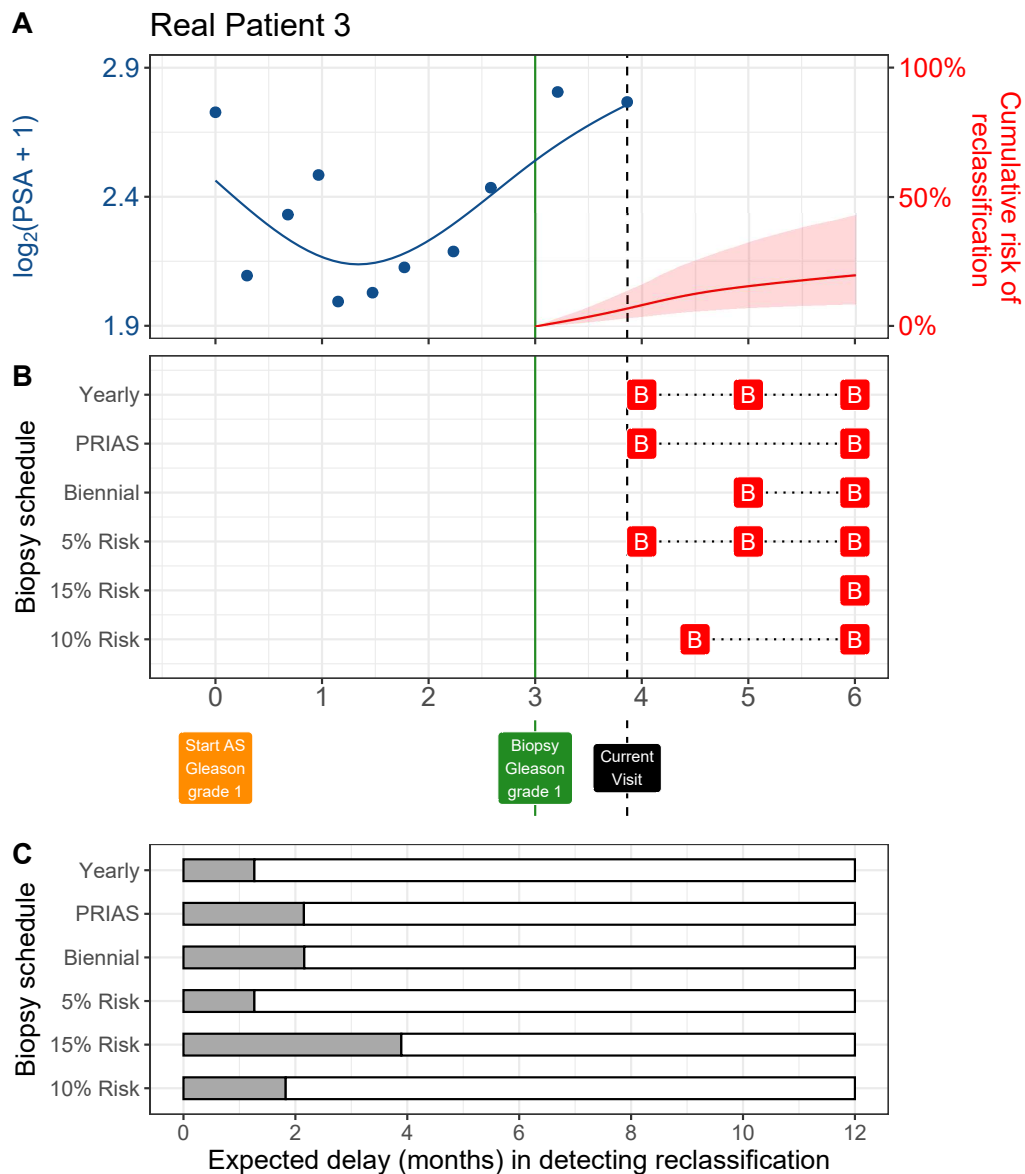


Figure 11: **Personalized and fixed schedules of biopsies for patient 3.** **Panel A:** shows the observed and fitted  $\log_2(\text{PSA} + 1)$  measurements (Equation 1), and the dynamic cumulative risk of reclassification (see Appendix B) over follow-up period. **Panel B** shows the personalized and fixed schedules of biopsies with a 'B' indicating times of biopsies. **Panel C** compares various schedules in terms of the expected delay in detection of reclassification if they are followed.

## Appendix D. Web Application for Practical Use of Personalized Schedule of Biopsies

We implemented our methodology in a web-application to assist patients and doctors in better decision making. It works on desktop as well as mobile devices. The cohorts that are currently supported in this web-application are PRIAS and the largest five cohorts from the GAP3 database [7]. These are the University of Toronto AS (Toronto), Johns Hopkins AS (Hopkins), Memorial Sloan Kettering Cancer Center AS (MSKCC), King's College London AS (KCL), and Michigan Urological Surgery Improvement Collaborative AS (MUSIC). The web-application is hosted at [https://emcbiostatistics.shinyapps.io/prias\\_biopsy\\_recommender/](https://emcbiostatistics.shinyapps.io/prias_biopsy_recommender/).

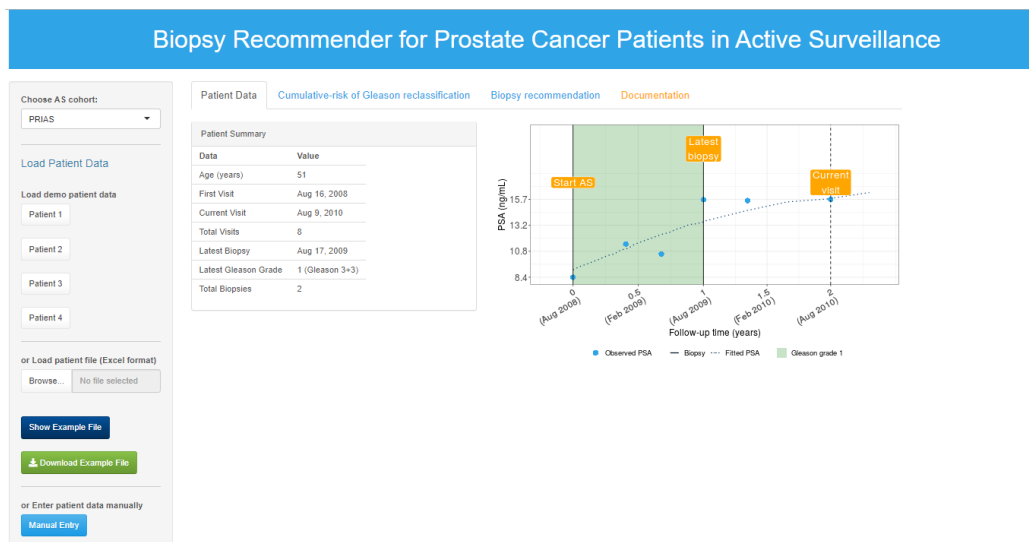


Figure 12: Landing page of the web-application. Panel on the left allows users to load patient data and panel on the right provides information. Patient data can be entered manually, or via Excel files. In addition, demo patient data is already uploaded to assist users in understanding the web-application.

## 201 Appendix E. Source Code

202 The R code for fitting the joint model to the PRIAS dataset, is at [https://github.com/anirudhtomer/prias/tree/master/src/clinical\\_gap3](https://github.com/anirudhtomer/prias/tree/master/src/clinical_gap3). We  
 203 refer to this location as ‘R\_HOME’ in the rest of this document.  
 204

### 205 *Appendix E.1. Fitting the Joint Model to the PRIAS dataset*

206 **Accessing the dataset:** The PRIAS dataset is not openly accessible.  
 207 However, access to the database can be requested via the contact links at  
 208 [www.prias-project.org](http://www.prias-project.org).  
 209

210 **Formatting the dataset:** This dataset however is in the so-called wide  
 211 format and also requires removal of incorrect entries. This can be done via  
 212 the R script `R_HOME/dataset_cleaning.R`. This will lead to two R objects,  
 213 namely ‘`prias_final.id`’ and ‘`prias_long_final`’. The ‘`prias_final.id`’ object con-  
 214 tains information about time of reclassification for PRIAS patients. The  
 215 ‘`prias_long_final`’ object contains longitudinal PSA measurements, the time  
 216 of biopsies and results of biopsies.  
 217

218 **Fitting the joint model:** We use a joint model for time to event and  
 219 longitudinal data to model the evolution of PSA measurements over time,  
 220 and to simultaneously model their association with the risk of reclassification.  
 221 The R package we use for this purpose is called **JMbayes** ([https://cran.r-](https://cran.r-project.org/web/packages/JMbayes/JMbayes.pdf)  
 222 [project.org/web/packages/JMbayes/JMbayes.pdf](https://cran.r-project.org/web/packages/JMbayes/JMbayes.pdf)). The API we use, how-  
 223 ever, are currently not hosted on CRAN, and can be found here: [https:](https://github.com/anirudhtomer/JMbayes)  
 224 [//github.com/anirudhtomer/JMbayes](https://github.com/anirudhtomer/JMbayes). The joint model can be fitted via  
 225 the script `R_HOME/analysis.R`. It takes roughly 6 hours to run on an Intel  
 226 core-i5 machine with 4 cores, and 8GB of RAM.

227 The graphs presented in the main manuscript, and the supplementary  
 228 material can be generated by the scripts in `R_HOME/plots/`.

### 229 *Appendix E.2. Validation of Predictions of Reclassification*

230 Validations can be done using the scripts `R_HOME/validation/auc_brier/`  
 231 `auc_calculator.R`, and `R_HOME/validation/auc_brier/gof_calculator.`  
 232 `R`. For external validation access to GAP3 database is required.

233 *Appendix E.3. Creating Personalized Schedules of Biopsies*

234     Once a joint model is fitted to the PRIAS dataset, personalized schedules  
235 of biopsies based on risk of reclassification for new patients can be devel-  
236 oped using the script `R_HOME/scheduleCreator.R`. This script also provides  
237 fixed biopsy schedules for the patients. In addition with each schedule, the  
238 expected delay in detection of reclassification is also provided.

239 *Appendix E.4. Source Code for Web Application*

240     Source for the shiny web application which provides biopsy schedules for  
241 patients can be found at `R_HOME/shinyapp`

## References

1. Epstein JI, Egevad L, Amin MB, Delahunt B, Srigley JR, Humphrey PA. The 2014 international society of urological pathology (isup) consensus conference on gleason grading of prostatic carcinoma. *The American journal of surgical pathology* 2016;40(2):244–52.
2. Pearson JD, Morrell CH, Landis PK, Carter HB, Brant LJ. Mixed-effects regression models for studying the natural history of prostate disease. *Statistics in Medicine* 1994;13(5-7):587–601.
3. Lin H, McCulloch CE, Turnbull BW, Slate EH, Clark LC. A latent class mixed model for analysing biomarker trajectories with irregularly scheduled observations. *Statistics in Medicine* 2000;19(10):1303–18.
4. De Boor C. A practical guide to splines; vol. 27. Springer-Verlag New York; 1978.
5. Eilers PH, Marx BD. Flexible smoothing with B-splines and penalties. *Statistical Science* 1996;11(2):89–121.
6. Turnbull BW. The empirical distribution function with arbitrarily grouped, censored and truncated data. *Journal of the Royal Statistical Society Series B (Methodological)* 1976;38(3):290–5.
7. Bruinsma SM, Zhang L, Roobol MJ, Bangma CH, Steyerberg EW, Nieboer D, Van Hemelrijck M, consortium MFGAPPCASG, Trock B, Ehdaie B, et al. The movember foundation’s gap3 cohort: a profile of the largest global prostate cancer active surveillance database to date. *BJU international* 2018;121(5):737–44.
8. Rizopoulos D. The R package JMbayes for fitting joint models for longitudinal and time-to-event data using MCMC. *Journal of Statistical Software* 2016;72(7):1–46.
9. Rizopoulos D, Molenberghs G, Lesaffre EM. Dynamic predictions with time-dependent covariates in survival analysis using joint modeling and landmarking. *Biometrical Journal* 2017;59(6):1261–76.
10. Steyerberg EW, Vickers AJ, Cook NR, Gerds T, Gonen M, Obuchowski N, Pencina MJ, Kattan MW. Assessing the performance of prediction

- models: a framework for some traditional and novel measures. *Epidemiology (Cambridge, Mass)* 2010;21(1):128.
11. Bokhorst LP, Alberts AR, Rannikko A, Valdagni R, Pickles T, Kakehi Y, Bangma CH, Roobol MJ, PRIAS study group . Compliance rates with the Prostate Cancer Research International Active Surveillance (PRIAS) protocol and disease reclassification in noncompliers. *European Urology* 2015;68(5):814–21.